

# Refractive-index matching enhanced polarization sensitive optical coherence tomography quantification in human brain tissue: supplement

CHAO J. LIU,<sup>1,6</sup>  WILLIAM AMMON,<sup>1</sup> ROBERT J. JONES,<sup>1</sup> JACKSON NOLAN,<sup>1</sup> RUOPENG WANG,<sup>1</sup> SHUAIBIN CHANG,<sup>2</sup>  MATTHEW P. FROSCH,<sup>3</sup> ANASTASIA YENDIKI,<sup>1</sup> DAVID A. BOAS,<sup>4</sup> CAROLINE MAGNAIN,<sup>1</sup> BRUCE FISCHL,<sup>1,5</sup> AND HUI WANG<sup>1,7</sup>

<sup>1</sup>Athinoula A. Martinos Center for Biomedical Imaging, Department of Radiology, Massachusetts General Hospital/Harvard Medical School, Charlestown, MA 02129, USA

<sup>2</sup>Department of Electrical and Computer Engineering, Boston University, Boston, MA 02215, USA

<sup>3</sup>C.S. Kubik Laboratory for Neuropathology, Massachusetts General Hospital/Harvard Medical School, Boston, MA 02114, USA

<sup>4</sup>Department of Biomedical Engineering, Boston University, Boston, MA 02215, USA

<sup>5</sup>MIT HST, Computer Science and AI Lab, Cambridge, MA 02139, USA

<sup>6</sup>cliu53@mgh.harvard.edu

<sup>7</sup>hwang47@mgh.harvard.edu

---

This supplement published with Optica Publishing Group on 15 December 2021 by The Authors under the terms of the [Creative Commons Attribution 4.0 License](#) in the format provided by the authors and unedited. Further distribution of this work must maintain attribution to the author(s) and the published article's title, journal citation, and DOI.

Supplement DOI: <https://doi.org/10.6084/m9.figshare.17086814>

Parent Article DOI: <https://doi.org/10.1364/BOE.443066>

## Supplemental Document

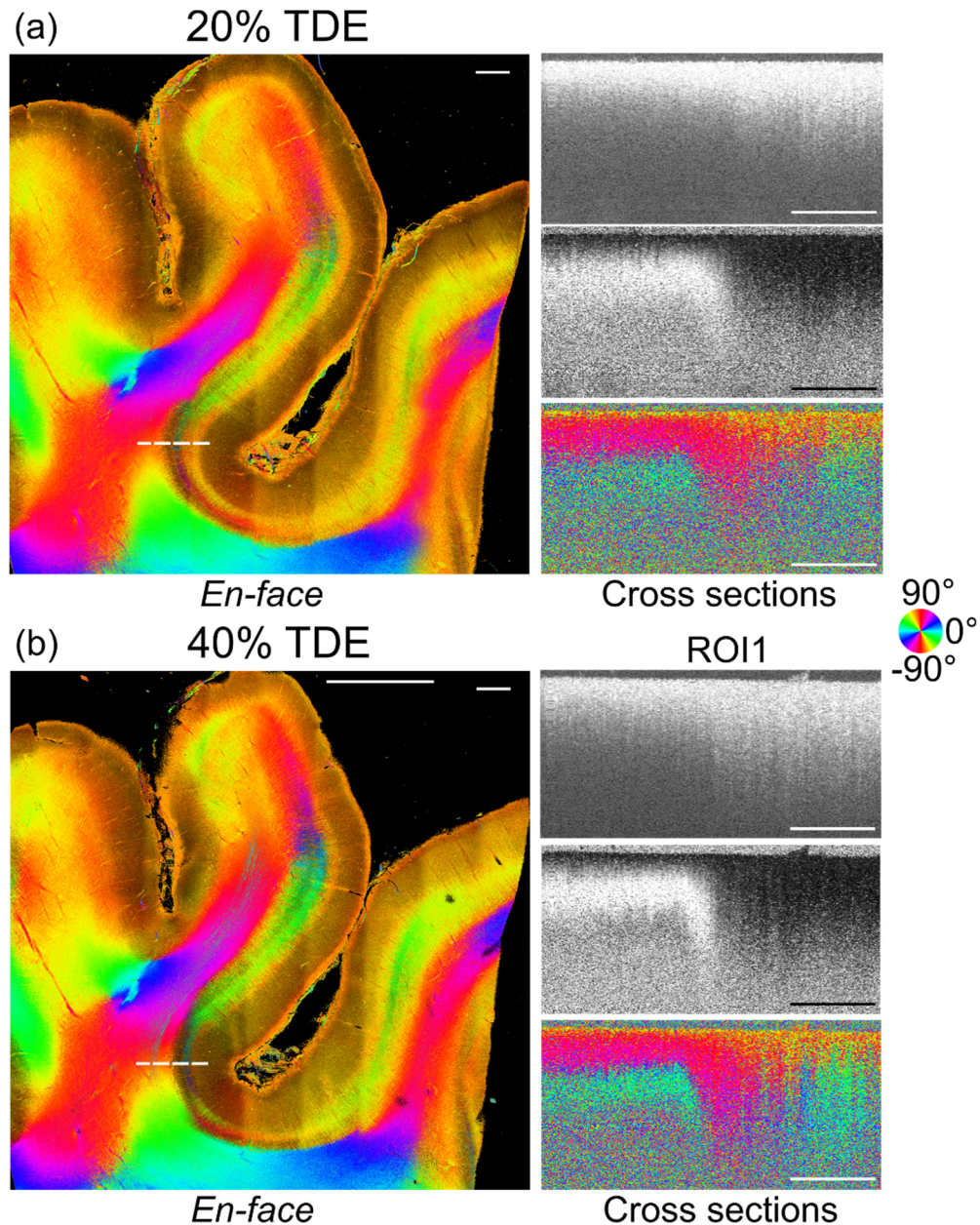


Fig. S1 PS-OCT images of human visual cortex in the occipital lobe *ex vivo* with 20% (a) and 40% TDE immersion (b), corresponding to Fig. 1. *En-face* optic axis orientation images by integrating 500  $\mu\text{m}$  in depth are shown on the left and cross-sectional images are shown on the right. The location of the cross-sectional images of intensity (35~75 dB), retardance (0~60 deg) and optic axis orientation (-90~90 deg) were indicated by the dashed line on the *en-face* orientation in (a) and (b), separately. For *en-face* orientation images, axis orientation values are color coded in HSV space as illustrated by the color wheel and the brightness is modulated by retardance. Scale bars: 1 mm.

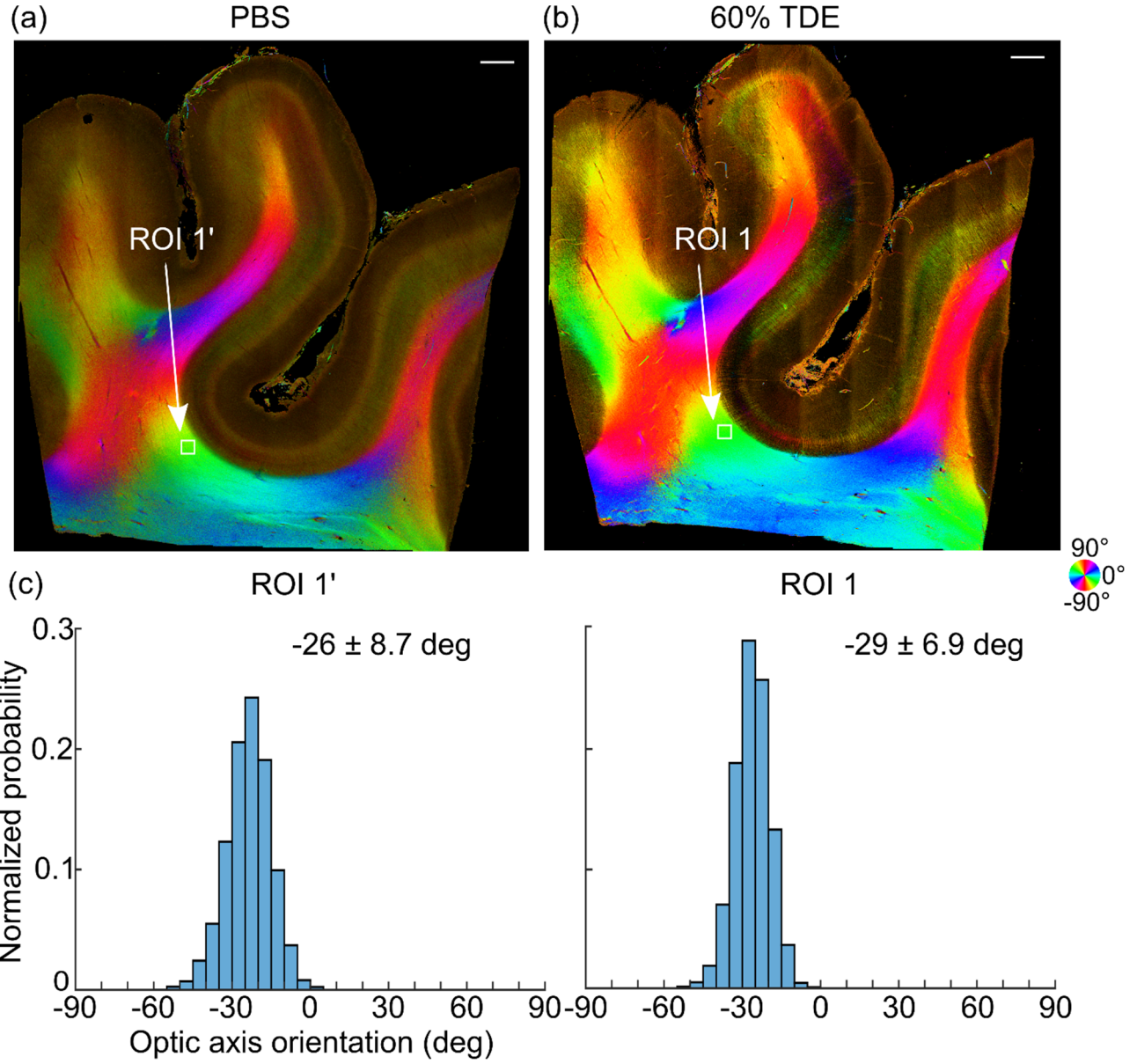


Fig. S2 *En-face* orientation images integrating 200  $\mu\text{m}$  in depth with PBS (a) and 60% TDE immersion (b), corresponding to Fig. 1.

(a) - (b) The axis orientation values are color coded in HSV space as illustrated by the color wheel and the brightness is modulated by retardance. Scale bars: 1 mm.

(c) The orientation distributions in the same 500  $\times$  500  $\mu\text{m}^2$  region labeled as ROI1' and ROI1 in (a) and (b), respectively. The averaged orientations are  $-26 \pm 8.7$  deg and  $-29 \pm 6.9$  deg with PBS and 60% TDE immersion.

Table S1. Apparent birefringence  $\Delta n$  measurements (mean $\pm$ S.D.) in the white matter with respect to TDE concentration at three depth intervals.

TDE concentration	0 – 200 $\mu\text{m}$	200 – 400 $\mu\text{m}$	400 – 600 $\mu\text{m}$
0%	0.15 $\pm$ 0.06 deg/ $\mu\text{m}$	0.04 $\pm$ 0.03 deg/ $\mu\text{m}$	0.04 $\pm$ 0.02 deg/ $\mu\text{m}$
20%	0.2 $\pm$ 0.07 deg/ $\mu\text{m}$	0.06 $\pm$ 0.04 deg/ $\mu\text{m}$	0.04 $\pm$ 0.03 deg/ $\mu\text{m}$
40%	0.25 $\pm$ 0.06 deg/ $\mu\text{m}$	0.13 $\pm$ 0.06 deg/ $\mu\text{m}$	0.04 $\pm$ 0.03 deg/ $\mu\text{m}$
60%	0.27 $\pm$ 0.09 deg/ $\mu\text{m}$	0.18 $\pm$ 0.08 deg/ $\mu\text{m}$	0.09 $\pm$ 0.06 deg/ $\mu\text{m}$

Table S2. Apparent birefringence  $\Delta n$  measurements (mean $\pm$ S.D.) in the gray matter with respect to TDE concentration at three depth intervals.

TDE concentration	0 – 200 $\mu\text{m}$	200 – 400 $\mu\text{m}$	400 – 600 $\mu\text{m}$
0%	0.023 $\pm$ 0.02 deg/ $\mu\text{m}$	0.08 $\pm$ 0.04 deg/ $\mu\text{m}$	0.04 $\pm$ 0.03 deg/ $\mu\text{m}$
20%	0.018 $\pm$ 0.01 deg/ $\mu\text{m}$	0.05 $\pm$ 0.03 deg/ $\mu\text{m}$	0.06 $\pm$ 0.03 deg/ $\mu\text{m}$
40%	0.019 $\pm$ 0.02 deg/ $\mu\text{m}$	0.04 $\pm$ 0.03 deg/ $\mu\text{m}$	0.06 $\pm$ 0.03 deg/ $\mu\text{m}$
60%	0.019 $\pm$ 0.02 deg/ $\mu\text{m}$	0.02 $\pm$ 0.02 deg/ $\mu\text{m}$	0.03 $\pm$ 0.02 deg/ $\mu\text{m}$

Table S3.  $Var_\theta$  measurements (mean $\pm$ S.D.) in the white matter with respect to TDE concentration at three depth intervals.

TDE concentration	0 – 200 $\mu\text{m}$	200 – 400 $\mu\text{m}$	400 – 600 $\mu\text{m}$
0%	26 $\pm$ 8 deg	58 $\pm$ 15 deg	59 $\pm$ 7 deg
20%	18 $\pm$ 5 deg	52 $\pm$ 18 deg	53 $\pm$ 9 deg
40%	16 $\pm$ 4 deg	38 $\pm$ 15 deg	54 $\pm$ 11 deg
60%	17 $\pm$ 5 deg	25 $\pm$ 13 deg	44 $\pm$ 19 deg

Table S4.  $Var_\theta$  measurements (mean $\pm$ S.D.) in the gray matter with respect to TDE concentration at three depth intervals.

TDE concentration	0 – 200 $\mu\text{m}$	200 – 400 $\mu\text{m}$	400 – 600 $\mu\text{m}$
0%	36 $\pm$ 13 deg	65 $\pm$ 12 deg	61 $\pm$ 8 deg
20%	27 $\pm$ 10 deg	52 $\pm$ 21 deg	60 $\pm$ 12 deg
40%	30 $\pm$ 15 deg	49 $\pm$ 20 deg	51 $\pm$ 16 deg
60%	32 $\pm$ 15 deg	40 $\pm$ 21 deg	40 $\pm$ 21 deg